SCIENTIFIC REPORTS

SUBJECT AREAS:
BEHAVIOUR
MODELLING
NEUROIMAGING
STATISTICS

Received
30 August 2011

Accepted
8 May 2012

Published
18 May 2012

Correspondence and requests for materials should be addressed to E.S.-K. (shokri@utdallas.edu)

# The Network Architecture of Cortical Processing in Visuo-spatial Reasoning

Ehsan Shokri-Kojori[1], Michael A. Motes[1,2], Bart Rypma[1,2] & Daniel C. Krawczyk[1,2]

[1]Center for BrainHealth, School of Behavioral and Brain Sciences, The University of Texas at Dallas, Dallas, TX, 75235-7205, USA, [2]Department of Psychiatry, University of Texas Southwestern Medical Center, Dallas, TX, 75390-9070, USA.

**Reasoning processes have been closely associated with prefrontal cortex (PFC), but specifically emerge from interactions among networks of brain regions. Yet it remains a challenge to integrate these brain-wide interactions in identifying the flow of processing emerging from sensory brain regions to abstract processing regions, particularly within PFC. Functional magnetic resonance imaging data were collected while participants performed a visuo-spatial reasoning task. We found increasing involvement of occipital and parietal regions together with caudal-rostral recruitment of PFC as stimulus dimensions increased. Brain-wide connectivity analysis revealed that interactions between primary visual and parietal regions predominantly influenced activity in frontal lobes. Caudal-to-rostral influences were found within left-PFC. Right-PFC showed evidence of rostral-to-caudal connectivity in addition to relatively independent influences from occipito-parietal cortices. In the context of hierarchical views of PFC organization, our results suggest that a caudal-to-rostral flow of processing may emerge within PFC in reasoning tasks with minimal top-down deductive requirements.**

Reasoning is a cognitive process associated with making logical inferences about experienced phenomena in the surrounding world. As an everyday driving example, imagine a traffic light turns yellow with some distance left to the intersection. Integrating this information indicates an upcoming red light, so the traffic rules require bringing the car to a stop. Reasoning involves making connections between sensory information, integrated features (i.e., perception of sensory information) and rules. Prefrontal cortex (PFC) plays a key role in mediating these interacting processes through interplay between multiple prefrontal areas and other, more specialized, cortical regions[1]. Thus, our approach to characterize PFC activity related to reasoning involved a brain-wide causal network analysis that combined functional connectivity characteristics with estimates of the distribution of activity between and within cortical regions. This approach allowed for the detection of the "processing flow" across the brain and, in particular, the direction of influence along the rostral-caudal axis of PFC in the context of reasoning tasks.

Recent studies have suggested an "abstractness" hierarchy along the rostral-caudal axis of PFC[2,3]. According to this top-down view, rostral areas are associated with more abstract processes such as maintenance of goals and rules, predominantly influencing caudal PFC activity that mediates domain-specific motor representations and sensory feature representations. In reasoning tasks, similar cognitive resources are expected to be engaged when the objective is to process and integrate sensory features (e.g. tracking and indentifying changes in a shape) and to verify certain rules (e.g. whether the shape rotates clockwise). However the flow of processing within PFC regions mediating the sequence of reasoning components has not yet been explored. More specifically, when performance rules must be verified on the basis of stimulus configurations, an overall caudal-to-rostral processing flow may be predicted, wherein domain-specific areas integrate stimulus features and communicate information to rule-processing regions.

Raven's Progressive Matrices (RPM) is a commonly used intelligence test that assesses human reasoning[4–6]. In RPM, participants are required to select an answer choice that best completes a progression of one or multiple rules among a series of visual items. Due to the multimodal nature of RPM[7] and the possibility of confounding variability in individuals' approaches to solving reasoning problems, reliable assessment of the contributing cognitive resources becomes extremely challenging. In response to these concerns, we designed a visuo-spatial reasoning task (VSRT) that required participants to perform a sequence of *sensory processing*, *feature integration*, and *rule verification* steps. For sensory processing, participants were asked to visually inspect the shapes presented within three panels in each trial. In addition, through feature integration, they had to identify change patterns across the panels (e.g., identifying a revolving shape). Finally, in the rule verification step, the identified patterns were compared against a collection of known rules (see Results and Methods for more details). This task enabled

examination of processing sequences involved at the *feature* level of visuo-spatial reasoning problems. Similar processing sequences would be involved in more abstract relational reasoning, wherein relationships between abstract representations (e.g., relational rules) emerging from processing of *stimulus features* are *integrated* and *verified*. Thus, the VSRT would be expected to engage basic processes common to a range of relational reasoning problems.

In contrast to RPM, participants were pre-trained on the set of task rules (i.e., allowable change patterns) to avoid recruitment of highly top-down and hard-to-administer processes involved in the generation of logical rules. The sequential nature of the VSRT enabled us to observe these reasoning components through the temporal order of corresponding neural responses. Further, the number of stimulus dimensions (i.e., spatial changes in visual objects) was parametrically varied, allowing us to track increasing responses within occipital and parietal regions (associated with visuo-spatial processing), as well as domain-specific areas (associated with feature integration) within hypothesized PFC hierarchies. We applied multivariate Granger causality (MGC) analysis to address the question of whether the predominant flow of processing is in a feed-backward (rostral-caudal) or a feed-forward (caudal-rostral) manner while controlling for top-down task aspects through minimizing rule generation requirements.

Furthermore, using this brain-wide causal analysis, we were able to distinguish the cascade of proximal inter-PFC influences, implying hierarchically processing regions, from alternative connectivity topologies, such as independent influences from remote parietal and occipital regions to PFC, as well as loops of bidirectional interactions among active brain areas. Finally, we made group comparisons based on speed of processing to investigate connectivity networks mediating efficient reasoning performance.

## Results

In each VSRT trial, participants viewed three simultaneously-presented frames. The left frame consisted of four shapes occupying different spatial positions. Each position was associated with one

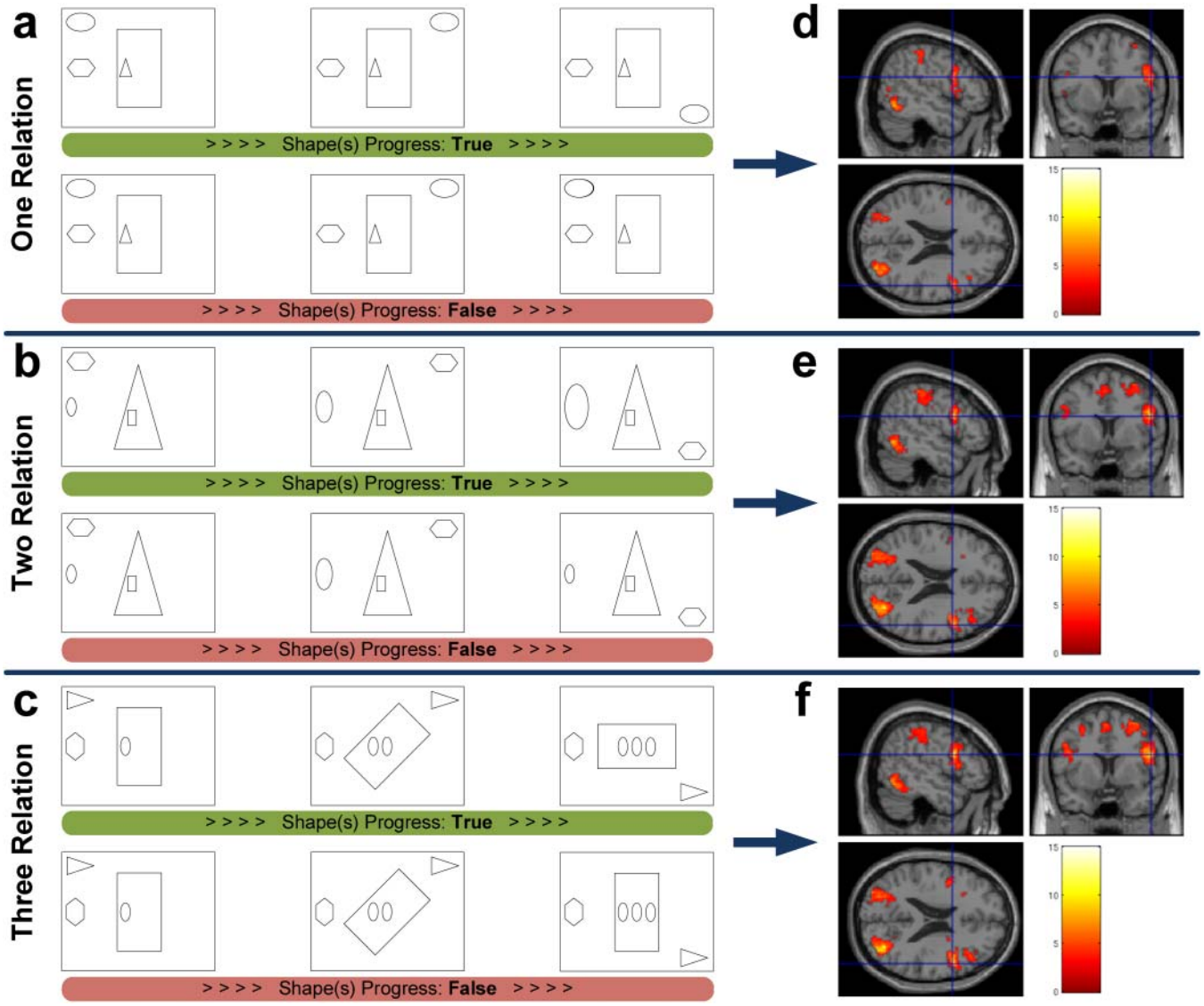


**Figure 1 | The VSRT and the associated brain activity.** Participants judged whether shapes changed across the 3 frames according to the following alteration rules: clockwise revolution for the shape in left upper corner, size increase for the left-side shape, multiplication for the center shape and clockwise rotation for the surrounding center shape. (a) One relation condition. The ellipsoid should continue revolving clockwise along the corners of the frame. (b) Two relation condition. The polygon should revolve clockwise and the ellipsoid should continue increasing in size. (c) Three relation condition. Together with the revolving triangle and multiplying ellipsoids, the surrounding rectangle should continue a clockwise rotation around the center. (d–f) Activation *t*-maps for one, two and three relations, respectively (brighter colors represent larger *t*-values, FDR, $P < 0.05$). More consistent recruitment of left caudal PFC is evident when relational complexity increases.

predefined alteration rule (Fig. 1). Proceeding from left to right, one, two or three of the shapes were altered so as to vary the relational complexity (Fig. 1a-c). A shape always began in one location and either remained the same or began to change in the second frame. Only if it had started to change in the second frame did it finish changing in the third frame. If all shapes completed their sequence of changes in the rightmost frame, the trial was considered to be "True" (half of the trials). Participants were instructed to respond to such trials by a right key press. In the other half of the trials, one of the shapes that had altered in position from the leftmost to the middle frame, returned to its original position in the rightmost frame. Participants were instructed to respond "False" to such trials by making a left key press. Prior to the functional magnetic resonance imaging (fMRI) session, participants were given instructions and examples showing possible types of allowable shape alterations.

Average task accuracy varied from 98% in the simplest condition to 95% and 92% at the higher complexity levels. Reaction time (RT) was more variable across participants and increased from 2137 ms to 2500 ms and 2744 ms, respectively, as the task complexity increased. A positive linear trend was observed in RT as relational complexity increased from level one to level three ($F_{1,57} = 15.18$, $P = 0.0003$). Our hypothesis was that the VSRT evoked cognitive processes similar to conventional reasoning paradigms (such as the RPM), but with a sequential task structure and without the open-ended deductive requirements of these paradigms. We compared VSRT and RPM performance (i.e., accuracy and RT) on an additional thirty-two participants outside the scanner (see Supplementary Methods). Significant correlations were observed between performance in each of the VSRT conditions and the RPM. These results supported our hypothesis that the VSRT conditions involved processes similar to those of conventional reasoning problems. Moreover, the strength of the performance correlations remained relatively unchanged, suggesting that similar cognitive processes are recruited across VSRT conditions. Though task conditions appear to tax similar cognitive processes, they had different durations of engagement indexed by changes in the mean RT.

Increasing the relational complexity (i.e., the number of independent shape alterations) was expected to modulate the neural responses to sensory processing, feature integration, and rule verification components. Functional regions of interest (ROIs) were extracted by investigating regions that exhibited a linear increase in activity as a function of task difficulty (i.e., contrasting activation maps of level-three complexity to level-one complexity). These ROIs included bilateral areas from inferior frontal, middle frontal, and posterior orbital gyri, as well as cingulate and inferior frontal sulci within PFC (Fig. 2a). ROIs within the caudate nucleus and the thalamus were also detected. Large clusters of activation within the occipital and the parietal lobes constituted a major portion of active voxels in the posterior areas of the brain. Throughout different VSRT conditions, only the quantity of manipulated stimulus features (i.e., the number of changing shapes) was altered while the complexity of rules was held constant. Thus, we predicted that the linear increase in RT (indexing "task-demand") would mostly reflect the extended recruitment of sensory processing and feature integration components rather than the rule verification processes. Thereby, "demand-sensitivity" of regions to modulation of these task components (i.e., sensory processing and feature integration) was determined by correlating RT with ROI *t*-values (indexing regressor reliability) calculated for different task conditions. ROIs with significant group-level correlations are shown in Fig. 2a. These regions are mostly left-sided within PFC (i.e. IFGpo and MFG). Cingulate sulcus, parietal, and occipital ROIs exhibited bilateral demand-sensitivity. These results are consistent with the functional role of caudal PFC, suggesting that demand-sensitive regions within left caudal-PFC mediate domain-specific processes such as feature integration. Moreover, consistent with specialization of occipital and parietal cortices, sensitivity of these ROIs to task-demand can be related to subsequent modulation of visuo-spatial sensory processing.

The manipulation of task complexity was not expected to engage a categorically different sequence of cognitive processes. This hypothesis was supported by the consistency in the pattern of correlations between the performance measures across task conditions and the RPM (see Supplementary Methods). Thus, the group-level connectivity analysis was performed on the fMRI time-series representing all task conditions. The results are summarized in Fig. 2a, where each arrowed line represents an individually reliable Granger causal influence in one direction. Bidirectional connections with significant connectivity in either direction (solid blue lines) were observed between bilateral MOG, bilateral IpS, and right IFGpo ROIs. These regions form a heavily interconnected right prefrontal-parietal-occipital (rPPO) loop previously associated with visuo-spatial processing[8,9]. Further, connectivity pathways within left and right PFC were examined. Caudal PFC activation (i.e., IFGpo and CS) in both hemispheres was influenced by occipital and parietal areas. Rostral PFC within the right hemisphere (i.e., IFS, IFGpt, and POG) showed evidence of similar occipital and parietal influences with minimal indication of local interconnectivity. In contrast, left rostral PFC regions (i.e., IFS and IFGpt) were influenced proximally by progressive caudal-to-rostral connections. Activity in left IFGpo predicted the activity in left IFGpt and activity in left CS predicted the activity in left IFS. Both left IFGpo and left IFGpt were established as demand-sensitive regions. To further examine the directionality of the identified group-level connections, the causal influences in both directions were contrasted within each ROI pair with significant connectivity, and the dominant direction of influence is shown in Supplementary Fig. S1. Almost all of the group-level connections, particularly along the rostral-caudal axis of PFC, survived the additional contrast analysis. Furthermore, the distinctiveness of the connectivity patterns between hemispheres was assessed through a contrast analysis between significant group-level connections and their homologous connections in the contralateral hemisphere (Supplementary Fig. S2). These results support a similar hemispheric distribution of connections, however, with the expectation of some connections found in left PFC (e.g., left IFGpo to left IFGpt).

Consistent with the hypothesized functional organization of PFC[2], the terminal rostral PFC areas may be associated with more abstract processing components, such as rule verification. Additionally, our behavioral data support a rule processing role for the rostral PFC, where activity in these regions was generally insensitive to the task-demand (as indexed by RT), given that the complexity of the rules was not manipulated across task conditions. The results suggest that the caudal-rostral organization may represent a series of hierarchically functioning regions, but only within the left hemisphere. By comparison, corresponding right PFC activity appears to represent relatively independent functional processes associated with visuo-spatial reasoning. The interhemispheric functional connectivity was mediated through bilateral Tp, CN and CS. The coordinates of MFG ROIs are within the range of frontal eye field (FEF) coordinates[10] (Supplementary Table S1). These MFG ROIs were mainly influenced by visuo-spatial representations within rPPO loop and activity in right IFGpo, together mediating the most demanding motor output (i.e., eye movements), but not from more anterior PFC regions.

The connectivity networks of fast and slow performers (based on a median split) were examined in order to dissociate connections contributing to reasoning speed. For fast performers, connections within left PFC and rPPO loop became significant (Fig. 2b). For slow performers, few influences within right PFC were detected, suggesting relatively less consistent recruitment of cortical networks across these participants (Fig. 2c). Furthermore, these results were complemented by directly contrasting connectivity measures across per-

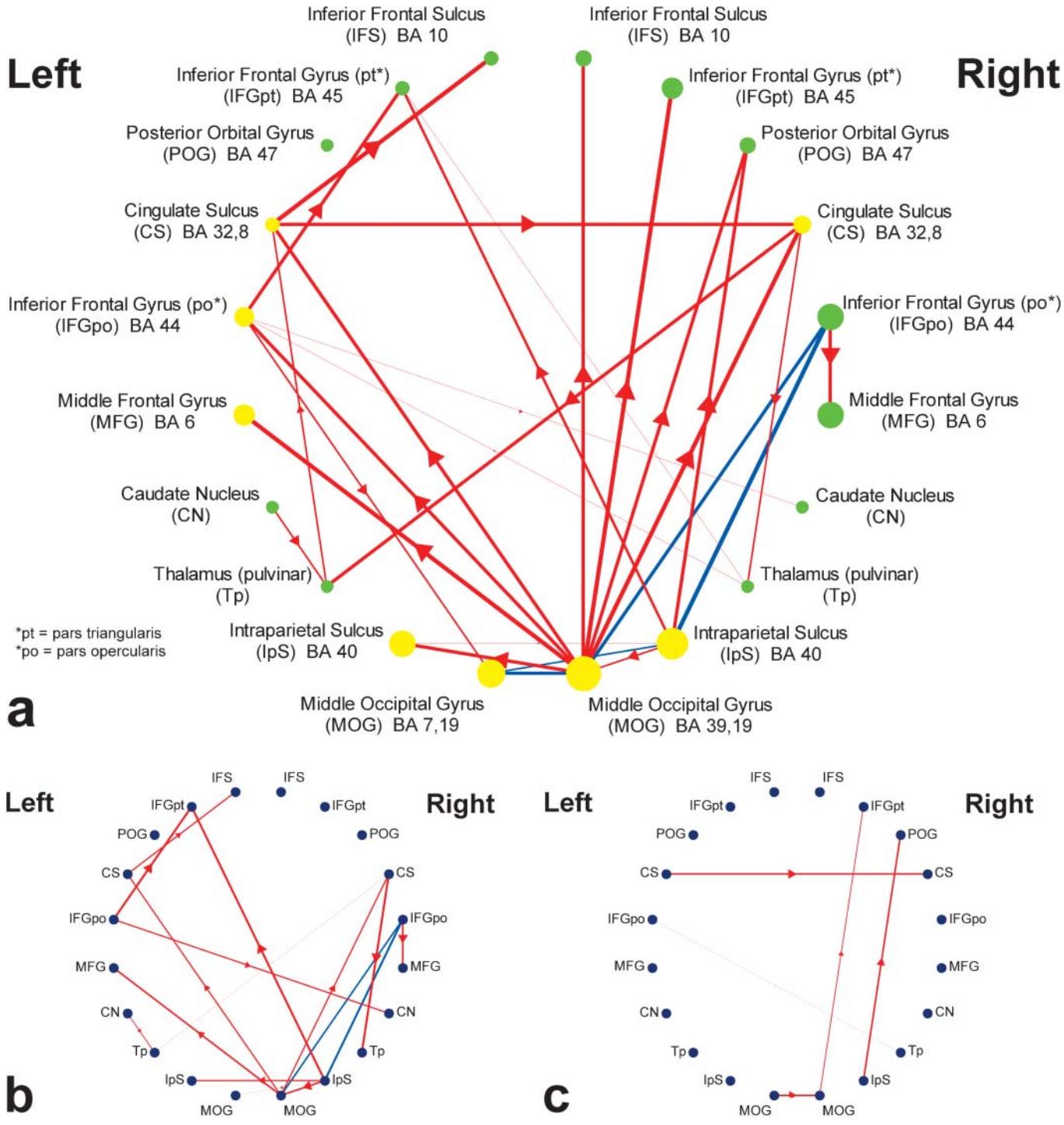


**Figure 2 | Topographical representations of causal connectivity maps.** ROIs are positioned based on their order along the coronal axis. (a) Group-level causal connectivity and sensitivity to task-demand. ROIs show regions with linear increase in activity in response to increased task complexity (FDR, $P < 0.05$). Yellow circles represent demand-sensitive ROIs where their activation significantly increased along with RT (FDR, $P < 0.05$). Green circles represent non-significant correlations with RT. The radius of the circles is proportional to the mean *t*-value of selected voxels within each ROI across all VSRT conditions. Directional influences are represented by red lines with thickness proportional to significance (FDR, $P < 0.05$). Blue lines represent significant bidirectional connections (FDR, $P < 0.05$). (b) Connectivity map of fast performers. Group-level connections were explored to detect those that are part of fast performers' connectivity network ($P < 0.01$). (c) Connectivity map of slow performers ($P < 0.01$).

formance groups. Accordingly, a collection of connections within the rPPO loop was found to be significantly stronger within the network of causal connections, but only when fast performers were compared to the slow performers (see Supplementary Fig. S1). Overall, these results suggest that efficient utilization of network components mediating sensory processing, feature integration, and rule verification (i.e., the rPPO loop and left PFC hierarchy) contribute to the speed of task performance.

## Discussion

Reasoning processes are jointly influenced by interactions between higher cognitive capabilities and the quality of incoming representa-

tions[11]. The extent to which higher cognition influences task performance has been termed the top-down aspect of a cognitive process. In contrast, when performance is affected by the quality of stimulus representations, the process is said to be mainly bottom-up. Functional mapping of these processes, central to PFC networks, has remained a difficult challenge from both neural and cognitive perspectives. From a neural perspective, massive anatomical interconnectivity among PFC regions and between the PFC and posterior cortical areas has been observed[12]. Predominantly feed-forward processing from posterior regions are shown to mediate bottom-up information processing, while feed-backward connections, particularly from the PFC to posterior areas, mediate top-down processing[13]. Further, PFC neurons tend to show highly flexible response properties[14,15]. From a cognitive perspective, top-down and bottom-up task components can be expected to differentially affect the flow of underlying neural processing, particularly within PFC. These competing influences can affect detection of the sequence of reasoning processes in performance conditions where both bottom-up and top-down components are emphasized. In order to overcome these confounding factors in observing the order of processing, we structured reasoning conditions where top-down task requirements were minimized (i.e., eliminating rule generation processes).

Generally, relational integration tasks require processing and integration of multiple relations and rules embedded in the stimulus[8]. In many cases, these problems are decomposable into individual relations that can be explored and processed independently before one can reach a final solution through the integration of all relational outcomes. The VSRT represents this property of relational reasoning problems, through systematically manipulating the number of independent relations, in an attempt to discern the neural bases of relation processing. In contrast to the RPM, the simplified and well-practiced task structure ensured a controlled and directed recruitment of the cognitive resources involved in sensory processing, feature integration, and rule verification.

Our brain-wide Granger causal connectivity approach adds to the picture provided by univariate activation maps to explore the sequence of processes involved in reasoning. Cortical interactions underlying the distribution of activities were incorporated as an essential element in characterizing PFC functions[16]. These cortical interactions can be utilized to track processing sequences emerging from more specialized regions (such as occipital and parietal cortices) and differentiating cortical activity based upon the incoming or outgoing influences within PFC regions.

We investigated the responsiveness of functional ROIs to the increased visuo-spatial processing demand in order to determine which brain regions are sensitive to subsequent increase in sensory processing and feature integration. Consistent with the prior literature investigating the neural basis of visuo-spatial reasoning[8,9,17], we found that when participants spent more time extracting and integrating visuo-spatial features (i.e., in more complex VSRT conditions), bilateral areas from occipital and parietal regions, along with left caudal PFC became significantly more responsive. However, considering our specific task design, rostral PFC activity did not show evidence of correlation with RT, suggesting relatively less association with sensory processing and feature integration components. The connectivity network of fast performers revealed two main networks contributing to efficient visuo-spatial reasoning: a right-sided visuo-spatial processing loop between prefrontal-parietal-occipital ROIs and left PFC caudal-to-rostral influences associated with feature integration and rule processing. Proximal interactions within PFC appeared to establish a hierarchical processing cascade, wherein domain-specific left caudal PFC areas (associated with sensory features) influenced the activity in rule-processing areas within left rostral PFC. However, some ROIs found within the PFC are somewhat ventral to regions previously established along the hierarchical PFC organization[2,21]. While our results still support the same organization pattern, we attribute these differences to the nonidentical processing modules engaged in our novel task compared to the tasks used in prior investigations of PFC hierarchies. The left-sided PFC network is consistent with recent findings indicating the dominant role of left rostrolateral PFC in relational integration[18,19]. The interactions from the posterior rPPO loop influenced most of the activity within right frontal lobe, which may be related to functions such as performance monitoring mechanisms associated with PFC[20].

These results may initially appear to be incompatible with cognitive control views, which emphasize greater rostral PFC influence on caudal regions in tasks that require top-down control, such as supervising steps involved in driving to the airport from one's home[2,21]. However, in practiced reasoning conditions with less rule ambiguity (i.e., reduced top-down demand), we have found evidence for both caudal-to-rostral and rostral-to-caudal processing within the PFC. The presence of caudal-to-rostral influences may be attributed to the fact that rule abstraction and planning of future actions were not strongly emphasized, which would likely stimulate more dominant rostral-to-caudal influences. Our results appear to indicate that in these reasoning conditions, there is a discernable temporal ordering of processing between posterior visuo-spatial representation and more anterior regions involved in feature integration and later rule verification identified in left PFC.

In summary, we have provided a framework within which the spatial distribution of cortical activity and brain-wide causal connections have been incorporated in characterizing regions mediating visuo-spatial reasoning. The present study shows the effectiveness of connectivity approaches to determine whether neural networks mediate task sub-processes through cascades of processing modules (e.g., the hierarchical influences within left PFC), loops of interacting regions (e.g., the rPPO loop), or independent influences from other brain regions (e.g., connections to right PFC). It should be noted that the functional role and representations within ROIs may not necessarily dictate the directionality of cortical influences. Depending on the nature of the task, similar regions might exhibit different strengths or directions of influence. Notably, a recent study on rule-learning processes has demonstrated that the bottom-up flow of information from caudal-to-rostral PFC during rule encoding stages can be reversed, if the presented rules were altered from novel to practiced sets[22]. However, the modulation of the respective processing flow during the response stage (i.e., rule execution), specifically in reasoning paradigms with different levels of rule ambiguity remains to be fully explored.

While, due to methodological limitations (e.g., insufficient continuous time points per block), our current design does not allow for comparisons of connections across different complexity levels, future research could complement our results by manipulating complexity of task sub-processes or bottom-up and top-down characteristics and examining subsequent modulations among cortical influences and estimates of activity. These observations would provide further insight into how cognitive demand leads to feed-forward and feedback flows of cortical processing in reasoning. The temporal and spatial resolution of fMRI limit detection of causal influences upon cortical activity (e.g., the outgoing connections from rostral PFC areas are not determined). Nonetheless, our results substantiate the application of methodologies required in studying brain-wide networks underlying the distribution of neural activity, mediating complex reasoning processes.

## Methods

**Participants.** Twenty healthy, right-handed, native English-speaking volunteers participated in the study. They ranged in age from 18 to 45 (11 females, mean age 27.5) and had normal or corrected vision. The experimental protocol received approval from the Institutional Review Boards of The University of Texas at Dallas and UT Southwestern Medical Center at Dallas. All participants provided informed consent to participate in accordance with the 1964 Declaration of Helsinki.

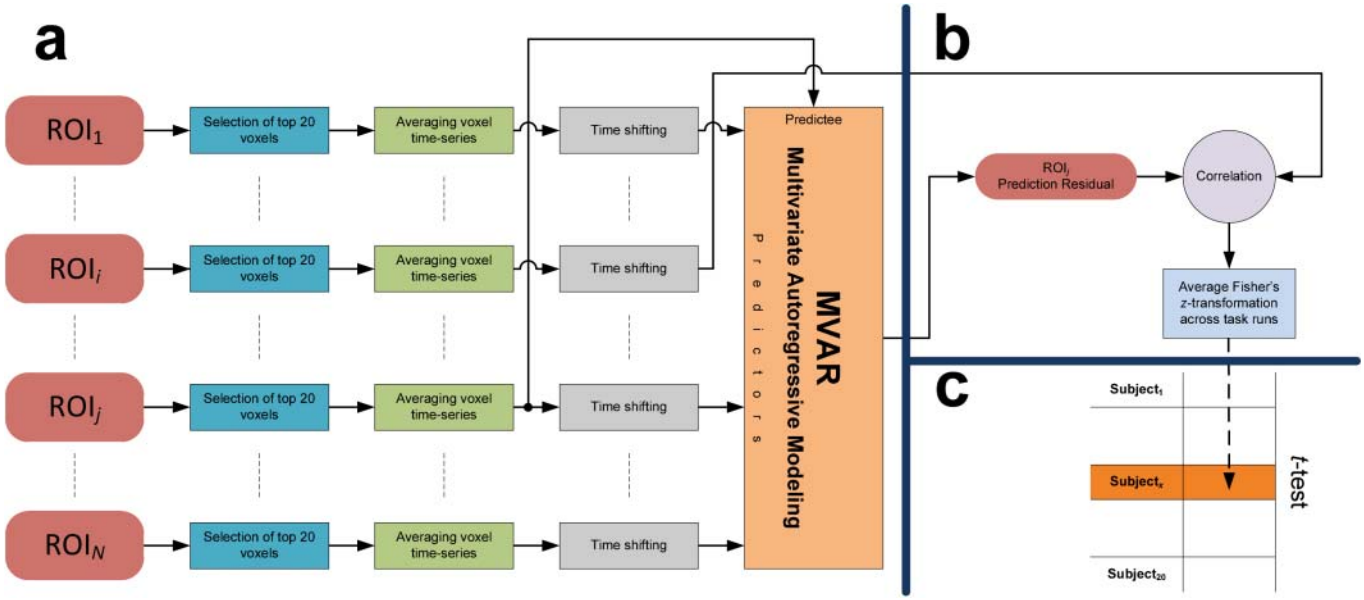


**Figure 3 | Group-level investigation of causal influence of ROI$_i$ on ROI$_j$ ($N = 20$).** (a) Schematic of the multivariate Granger causality (MGC) at the subject-level (Subject$_x$). Initially, the predictability components of other possible interacting regions (except ROI$_i$) were removed using multivariate auto regressive modeling (MVAR). (b) The residual signal was correlated with lagged time-series from ROI$_i$ to obtain the parameter estimate for unique causal influence of ROI$_i$ on ROI$_j$. (c) Significant causal influences were then determined using a two tailed *t*-test comparing the mean of Fisher's *z*-transformed correlations against zero (FDR, $P < 0.05$).

**The visuo-spatial reasoning task (VSRT).** The VSRT consisted of 96 trials varying in number of relations (1 to 3) and validity ("True" or "False") which were acquired in 2 runs, each consisting of 6 blocks of trials. Each block corresponded to one of the three problem types (1, 2, or 3 relations) consisting of 8 trials. The assignment of different shapes (e.g., triangle or ellipsoid) to spatial positions (e.g., center or left upper corner) was counterbalanced throughout VSRT trials. One of the four shapes always remained stationary to be considered as a reference across the three frames. The three frames within each trial were shown simultaneously to minimize the working memory load of different relational complexity levels. An introductory slide was shown for 6 seconds before the beginning of each block to inform the participants about the relational complexity level of the block. Within each trial, three frames were displayed for 5 seconds, with a 1-second fixation point between trials. Participants were instructed to respond within the 5-second display period and both accuracy and speed were emphasized. Blocks were positioned in a pseudo-random order to reduce collinearity between task regressors.

**Functional MRI data acquisition and processing.** Functional images were acquired using a 3T Philips MRI scanner with a gradient echo-planar sequence sensitive to BOLD contrast (TR = 2000 ms, TE = 30 ms, flip angle = 70°). Each volume consisted of 36 tilted axial slices (4 mm thick, no gap) that provided nearly whole brain coverage. Participants viewed the projected stimulus through a mirror above the receiving coil. Anatomical T1-weighted images were acquired in the following setup: TE = 3.76 ms, slice thickness = 1 mm, no gap, flip angle = 12°. Head motion was limited using foam head padding. Data processing was performed using Statistical Parametric Mapping Software (SPM5; Statistical Parametric Mapping; Wellcome Trust Centre for Neuroimaging, http://www.fil.ion.ucl.ac.uk/spm) run in MATLAB 7.4 (http://www.mathworks.com). Slice-timing correction was performed using sinc-interpolation to adjust for different acquisition time of slices. EPI images were realigned to the first volume of acquisition to correct for subject movement effects. Anatomical images were coregistered to the realigned EPI images. Normalization was performed by initially segmenting the coregistered anatomical brain into gray matter, white matter, and CSF. Then, nonlinear warping was applied to register individual brains into the MNI space[23]. The transformation derived from spatial normalization of the anatomical image was applied to the functional volumes to bring them into standardized MNI space.

Voxel-level data analysis was performed to assess activation patterns within the brain during different task conditions. Boxcar functions were created to represent the onset and duration of trials within the task blocks. Boxcar functions were convolved with the canonical HRF function to generate response estimates of each task condition. The resulting estimates, together with motion correction parameters, were used as regressors in the General Linear Model (GLM) analysis[24]. Brain areas significant at the group-level were detected by contrasting the parameter estimates of three to one relational complexity (i.e., the voxel-wise linear trend analysis of relational complexity, Supplementary Fig. S3). Based on this contrast map, twenty functional ROIs, at least 20 mm apart, were identified (Fig. 2a, Supplementary Table S3). To compensate for anatomical variability across participants and to ensure that only task-relevant voxels were considered in the analyses, we searched for most significant subject-level voxels within all ROIs. Accordingly, cubic search spaces ($20\times20\times20$ mm$^3$) were positioned on the peaks of group-level activations for all extracted ROIs with no overlapping spaces. For each participant, a cluster of top 20 significant voxels within each cubic ROI was selected for further data processing.

**Correlation between brain activations and reaction times.** In order to examine the effect of varying visuo-spatial task-demand on activity within ROIs, correlation coefficients between subject RT (i.e., mean RT per relational complexity level) and ROI activity (i.e., the mean *t*-value per relational complexity level) were obtained. Group-level analysis was performed by applying *t*-tests on the *z*-transformed correlation coefficients (Supplementary Fig. S4). ROIs with significant correlations are shown by yellow colored circles in Fig. 2a.

**Multivariate Granger causality analysis.** Multivariate Granger causality (MGC) analysis is a useful technique in detection of causal relations between multiple time-varying processes. Given that cognitive functions are mediated by neural interactions within and between active cortical and sub-cortical regions, MGC analysis can be applied in exploring these brain-wide causal interactions[25,26]. This approach, when applied to a network of ROIs, enables observation of unique and directional causal influences based on the temporal precedence of activity. In contrast to correlational connectivity approaches, MGC is capable of revealing driving sources for regions with similar activity, that are considered to be connected in the correlational approaches. Moreover, unlike other causality analysis techniques, such as structural equation modeling[27] and dynamic causal modeling[28], MGC is exploratory in nature, in that it does not require any presumption of connectivity patterns. This technique is based on identifying predictability properties of time-series representing regional hemodynamic responses throughout a cognitive task. Specifically, if inclusion of past time-series from a particular originating region uniquely improves the prediction of present activity within a target region (i.e., reducing the prediction error), then the originating region is inferred to have a Granger causal influence on the target region[29,30]. In this study, causal connectivity was analyzed to determine regional associations by specifying areas that influence each other more than other brain regions (see Supplementary Methods). The MGC method was applied to the preprocessed fMRI time-series averaged over subject-specific voxels within the functional ROIs. The preprocessing steps before applying the connectivity analysis included motion correction, slice-timing correction, and spatial normalization. After detrending the voxel time-series in each run[25], the MGC analysis was performed on the runs separately, and the resulting Fisher's *z*-values were averaged across the task runs to generate an estimate of causal correlations for each direction for a given ROI pair when other possible causal effects were partialled out (Fig. 3a&b). The MGC was adapted for group-level comparisons to investigate consistent cortical networks across participants mediating visuo-spatial reasoning (Fig. 3c).

1. Tomita, H., Ohbayashi, M., Nakahara, K., Hasegawa, I. & Miyashita, Y. Top-down signal from prefrontal cortex in executive control of memory retrieval. *Nature* **401**, 699–703 (1999).

2. Badre, D. & D'Esposito, M. Is the rostro-caudal axis of the frontal lobe hierarchical? *Nat. Rev. Neurosci.* **10**, 659–669 (2009).
3. Koechlin, E. & Summerfield, C. An information theoretical approach to prefrontal executive function. *Trends Cogn. Sci.* **11**, 229–235 (2007).
4. Raven, J. C., Court, J. H. & Raven, J. *Manual for Raven's Progressive Matrices and Vocabulary Scales* (Lewis, London, 1988).
5. Prabhakaran, V., Smith, J., Desmond, J., Glover, G. & Gabrieli, J. Neural substrates of fluid reasoning: An fMRI study of neocortical activation during performance of the Raven's Progressive Matrices Test. *Cogn. Psychol.* **33**, 43–63 (1997).
6. Perfetti, B., Saggino, A., Ferretti, A., Caulo, M., Romani, GL. & Onofrj, M. Differential patterns of cortical activation as a function of fluid reasoning complexity. *Hum. Brain. Mapp.* **30**, 497–510 (2009).
7. Snow, R. & Lohman, D. Toward a theory of cognitive aptitude for learning from instruction. *J. Ed. Psych.* **76**, 347–376 (1984).
8. Christoff, K. *et al*. Rostrolateral prefrontal cortex involvement in relational integration during reasoning. *Neuroimage* **14**, 1136–1149 (2001).
9. Prabhakaran, V., Narayanan, K., Zhao, Z. & Gabrieli, J. Integration of diverse information in working memory within the frontal lobe. *Nat. Neurosci.* **3**, 85–90 (2000).
10. Paus, T. Location and function of the human frontal eye-field: A selective review. *Neuropsychologia* **4**, 475–483 (1996).
11. Norman, D. & Bobrow, D. On data-limited and resource-limited processes. *Cogn. Psychol.* **7**, 44–64 (1975).
12. Petrides, M. & Pandya, D. Dorsolateral prefrontal cortex: comparative cytoarchitectonic analysis in the human and the macaque brain and corticocortical connection patterns. *Eur. J. Neurosci.* **11**, 1011–1036 (1999).
13. Miller, B. & D'Esposito, M. Searching for "the top" in top-down control. *Neuron* **48**, 535–538 (2005).
14. Wallis, J., Anderson, K. & Miller, E. Single neurons in prefrontal cortex encode abstract rules. *Nature* **21**, 953–956 (2001).
15. Miller, E., Freedman, D. & Wallis, J. The Prefrontal Cortex: Categories, Concepts and Cognition. *Philos. Trans. R. Soc. Lond. B Biol. Sci.* **357**, 1123–1136 (2002).
16. Fuster, J. The cognit: a network model of cortical representation. *Int. J. Psychophysiol* **60**, 125–132 (2006).
17. Kroger, J., Sabb, F., Fales, C., Bookheimer, S., Cohen, M. & Holyoak, K. Recruitment of anterior dorsolateral prefrontal cortex in human reasoning: a parametric study of relational complexity. *Cereb. Cortex* **12**, 477–485 (2002).
18. Bunge, S., Helskog, E. & Wendelken, C. Left, but not right, rostrolateral prefrontal cortex meets a stringent test of the relational integration hypothesis. *Neuroimage* **46**, 338–342 (2009).
19. Hampshire, A., Thompson, R., Duncan, J. & Owen, A. Lateral prefrontal cortex subregions make dissociable contributions during fluid reasoning. *Cereb. Cortex* **21**, 1–10 (2010).
20. Petrides, M. Impairments on nonspatial self-ordered and externally ordered working memory tasks after lesions of the mid-dorsal part of the lateral frontal cortex in the monkey. *J. Neurosci.* **15**, 359–375 (1995).
21. Koechlin, E., Ody, C. & Kouneiher, F. The architecture of cognitive control in the human prefrontal cortex. *Science* **14**, 1181–1185 (2003).
22. Cole, M., Bagic, A., Kass, R. & Schneider, W. Prefrontal dynamics underlying rapid instructed task learning reverse with practice. *J. Neurosci.* **30**, 14245–14254 (2010).
23. Ashburner, J. & Friston, K. Nonlinear spatial normalization using basis functions. *Hum. Brain Mapp.* **7**, 254–266 (1999).
24. Friston, K., Holmes, A., Worsley, K., Poline, J. P., Frith, C. & Frackowiak, R. Statistical parametric maps in functional imaging: a general linear approach. *Hum. Brain Mapp.* **2**, 189–210 (1995).
25. Seth, A. A MATLAB toolbox for Granger causal connectivity analysis. *J. Neurosci. Methods* **186**, 262–273 (2009).
26. Roebroeck, A., Formisano, E. & Goebel, R. Mapping directed influence over the brain using Granger causality and fMRI. *Neuroimage* **25**, 230–242 (2005).
27. Pearl, J. *Causality: Models, Reasoning, and Inference* (Cambridge University Press, New York, 2000).
28. Friston, K., Harrison, L. & Penny, W. Dynamic causal modelling. *Neuroimage* **19**, 1273–1302 (2003).
29. Granger, C. Investigating causal relations by econometric models and cross-spectral methods. *Econometrica* **37**, 424–438 (1969).
30. Geweke, J. Measures of conditional linear-dependence and feedback between time-series. *J. Am. Stat. Assoc.* **79**, 907–915 (1984).


## Acknowledgments

The authors thank A. O'Toole and I. J. Bennett for valuable comments. We also thank M. McClelland and C. Donovan for assistance in data collection.

## Author contributions

E. S.-K. analyzed the data and wrote the manuscript. M. A. M. and B. R. designed the experiment and edited the manuscript. D. C. K. designed the experiment and wrote the manuscript.

## Additional information

**Supplementary information** accompanies this paper at http://www.nature.com/scientificreports

**Competing financial interests:** The authors declare no competing financial interests.



**How to cite this article:** Shokri-Kojori, E., Motes, M.A., Rypma, B. & Krawczyk, D.C. The Network Architecture of Cortical Processing in Visuo-spatial Reasoning. *Sci. Rep.* **2**, 411; DOI:10.1038/srep00411 (2012).